자원환경지질, 제42권, 제1호, 001-008, 2009
Econ. Environ. Geol., 42(1), 001-008, 2009

Geochemical Environments of Copper-bearing Ore Mineralization in the Haman Mineralized Area

Sang-Hoon Choi*

Department of Earth & Environmental Sciences, Chungbuk National University, Cheongju 361-763, Korea

함안지역 함 동 광화작용의 지화학적 환경

최상훈*

충북대학교 지구환경과학과

함안광화대는 한반도 남동부 백악기 경상퇴적분지 내에 위치한다. 함안광화대에는 함동 다금속 열수 맥상 광화작용이 진행되어, 함동광물을 포함한 황화광물들과 철산화광물 및 황염광물 등이 열극을 충진하여 발달한 전기석, 석영 및 탄산염광물 맥 내에 산출한다. 본 광화대 내에는 군북, 제일군북 및 함안 광상 등이 분포한다. 광화대의 광화작용은 함철 및 함동 광화작용이 주로 진행된 광화 I 기와 주된 동광화작용이 진행되어 황화광물과 황염광물이 산출하는 광화 II 기 및 금속광물의 산출이 이루어지지 않은 방해석맥으로 이루어진 광화 III 기로 구분된다. 광물공생관계와 광물의 지화학적 조성특성 등이 고려된 열역학적 연구결과 주된 함동광물인 황동석의 침전은 약 350°C 에서 시작되어 약 250°C 까지 진행되었다. 동은 주로 염화복합체로 이동되었으며, 상기 온도의 냉각과정에 수반된 지화학적 환경요인 (fs_2, fo_2, pH 등) 들의 변화에 의한 함동 염화복합체의 용해도 감소에 의하여 침전되었다.

주요어 : 함안광화대, 동광화작용, 광물조합, 용해도, 함동염화복합체

The Haman mineralized area is located within the Cretaceous Gyeongsang Basin along the southeastern part of the Korean peninsula. Almost all occurrences in the Haman area are representative of copper-bearing polymetallic hydrothermal vein-type mineralization. Within the area are a number of fissure-filling hydrothermal veins which contain tourmaline, quartz and carbonates with Fe-oxide, base-metal sulfide and sulfosalt minerals. The Gunbuk, Jeilgunbuk and Haman mines are each located on such veins. The ore and gangue mineral paragenesis can be divided into three distinct stages: Stage I, tourmaline + quartz + Fe-Cu ore mineralization; Stage II, quartz + sulfides + sulfosalts + carbonates; Stage III, barren calcite. Equilibrium thermodynamic data combined with mineral paragenesis indicate that copper minerals precipitated mainly within a temperature range of 350°C to 250°C. During early mineralization at 350°C, significant amounts of copper (10^3 to 10^2 ppm) could be dissolved in weakly acid NaCl solutions. For late mineralization at 250°C, about 10^0 to 10^{-1} ppm copper could be dissolved. Equilibrium thermodynamic interpretation indicates that the copper in the Haman-Gunbuk systems could have been transported as a chloride complex and the copper precipitation occurred as a result of cooling accompanied by changes in the geochemical environments (fs_2, fo_2, pH, etc.) resulting in decrease of solubility of copper chloride complexes.

Key words : Haman mineralized area, copper mineralization, mineral assemblage, solubility, copper chloride complexes

1. Introduction

Most copper-bearing vein deposits in Korea are associated intimately with major periods of Cretaceous granitic magmatism (Sillitoe, 1980; Jin *et al.*, 1982; Sato *et al.*, 1981; So *et al.*, 1985; Choi *et al.*, 1994; Yun *et al.*, 1996; So *et al.*, 1997; Choi *et al.*, 1998; Heo *et al.*, 2001) and occur in the Gyeongnam mineralized province in the southern portion of the Gyeongsang Basin. The Haman-Gunbuk

*Corresponding author: cshoon@chungbuk.ac.kr

copper mineralized area is one of several important copper mineralized areas within the Gyeongnam province. Detailed mineral assemblages and paragenesis, and fluid composition and evolution of the Cu-bearing hydrothermal deposits in the province are spatially different. This may indicate that origins and evolutions of hydrothermal fluids within the Gyeongnam province varied in time and space due to differences in wall-rocks and granitic magmatism. Sillitoe (1980) documented porphyry-type mineralization in the province.

Almost all occurrences in the Haman area are representative of copper-bearing polymetallic hydrothermal vein-type mineralization. Within the area are a number of fissure-filling hydrothermal veins which contain tourmaline, quartz and carbonates with Fe-oxide, base-metal sulfide and sulfosalt minerals. The Gunbuk, Jeilgunbuk and Haman mines are each located on such veins.

Fluid inclusion and stable isotope study of copper mineralization in the area had been extensively studied by the author and co-workers (Heo *et al.*, 2003).

In this paper, I determine the geochemical environments of copper-bearing ore mineralization in the Haman area.

2. Geology and Ore Veins

The Haman area is located approximately 290 km southeast of Seoul along the southwestern margin of the Gyeongsang Basin (Fig. 1). Geology of the area consists of sedimentary rocks of the Middle Cretaceous Chindong Formation of the Hayang Group, andesite of the Upper Cretaceous Yucheon Group and a younger granodiorite (Fig. 1).

Rocks of the Cretaceous Hayang Group, the middle unit of the Gyeongsang Supergroup, consist of a sequence of sedimentary rocks with a few intercalated volcanic horizons. The Chindong Formation represents the upper portion of the Group and composed predominantly of dark gray shale, mudstone and sandstone. The Chindong Formation is intruded by a granodiorite phase of the Chindong granite.

The Yucheon Group is composed of volcanic and sedimentary rocks. It is characterized by the dominance of volcanic rocks in contrast to the unconformably underlying Hayang Group. Andesite is the only rock of the Yucheon Group that occurs in the mine area and is found as small masses and intrusions (or extrusions) within sedimentary rocks of the Chindong Formation.

Granodiorite is considered to be related genetically to hydrothermal systems in the area and is a phase of the Chindong Granites. The small stocks of the Chindong Granites occurring in the area are mainly medium-grained granodiorite. The granodiorite is composed mainly of plagioclase, orthoclase, quartz, hornblende and biotite with minor pyroxene, chlorite, sphene, tourmaline, apatite, zircon, rutile, magnetite and pyrite. Basic and acidic dikes of Cretaceous age intrude sedimentary rocks and granodiorite in the northern portion of the mine area.

Within the mine area is an extensive fault system which can be separated into two sets, one striking NW and another striking NE, both with high dip angles obliquely crosscutting sedimentary rock structures.

Within the Haman-Gunbuk area are a number of hydrothermal copper-bearing quartz and calcite veins formed by narrow open-space filling of parallel and subparallel faults (shear zones) striking approximately N-S and NW-SE (rarely NE-SW). Veins are developed mainly in sedimentary rocks surrounding the granodiorite mass in the center in the mining area, though some veins occur in the granodiorite.

Veins show textural evidence of open-space filling (internal mineral zonation), extend several hundred meters along strike and vary in width from $\approx$ 1cm to $\approx$ 150cm, displaying repeated pinching and swelling along strike and dip directions. Veins consist mainly of tourmaline and grey to milky white quartz with Fe-oxides, base-metal sulfides, sulfosalts and carbonates. Ores in the veins are massive, brecciated and banded. Fe-oxides and tourmaline occur mainly as massive bands in the hanging-wall or foot-wall side of veins.

3. Mineralogy

Mineralogical data of the Haman mineralized area (mineralization stages, mineralogy and mineral assemblages, and chemical compositions) have been published (Heo *et al*, 2003). In this section, I summarize the results.

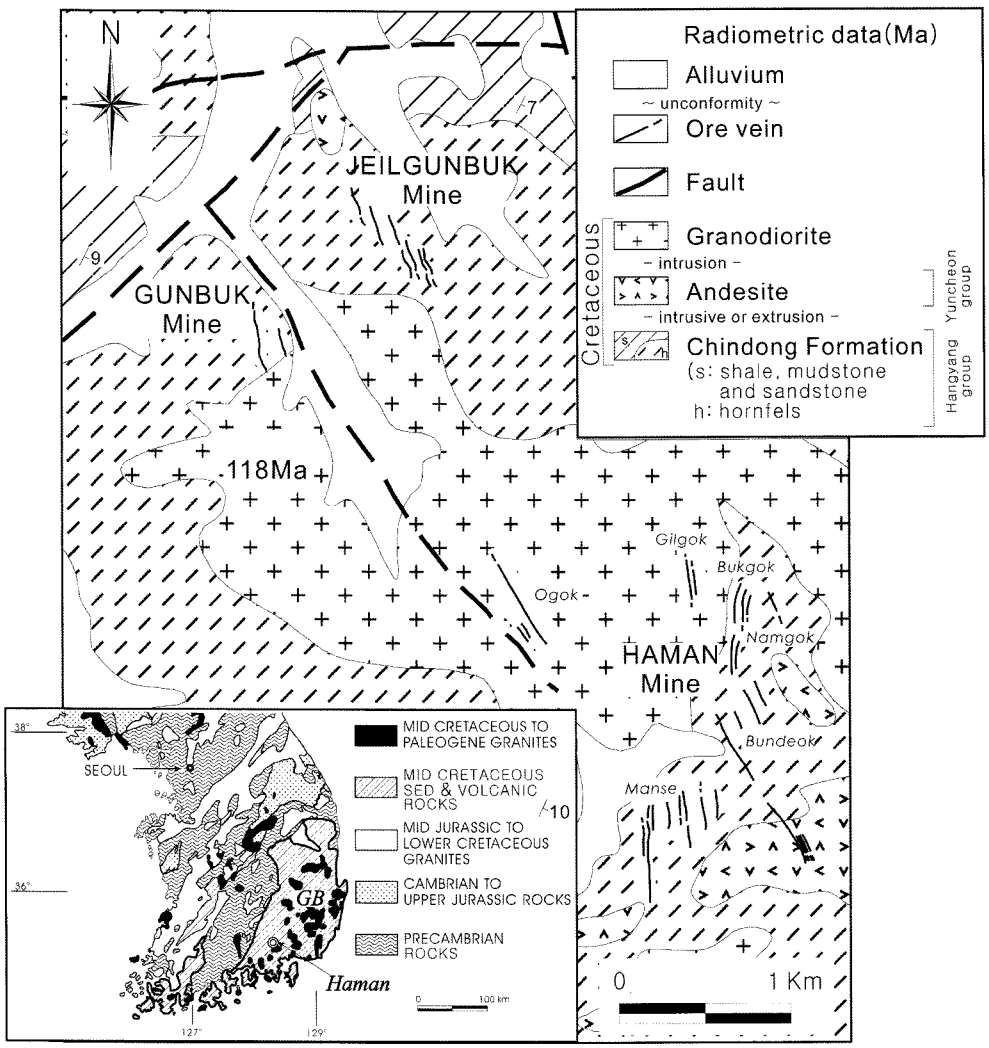

Fig. 1. Simplified geologic map of the Republic of Korea shows the location of the Human mineralized area *(Human)* and Gyeongsang basin *(GB)*.

Mineralogy of all the orebodies of the Haman mineralized area is complex. Tourmaline, quartz, carbonates, Fe-oxide, sulfide and sulfosalt minerals were deposited as open-space fillings. Chalcopyrite is the most abundant of the sulfide minerals and is accompanied by pyrite, arsenopyrite, pyrrhotite, marcasite, sphalerite and galena, together with minor electrum, tetrahedrite, native bismuth, polybasite, chalcocite and goethite. All minerals are primary with the exception of marcasite and goethite, which I suspect are formed by supergene processes. Mineralization in the area is characterized by several textural varieties (massive, brecciated and banded) which are infrequently mixed, resulting in complex textures.

Textural relationships indicate that veins were formed in three mineralization stages, separated by fracturing and brecciation events: stage I, tourmaline-Fe-oxide; stage II, main sulfide mineralization; stage III, late calcite. Generalized paragenetic sequence of vein minerals is summarized in Figure 2.

Stage I consists mainly of silicates and Fe-oxides with minor sulfides and is divisible into Fe stage, during which tourmaline plus the majority of the hematite and magnetite were deposited, and Fe-Cu stage, which is represented by quartz, magnetite,

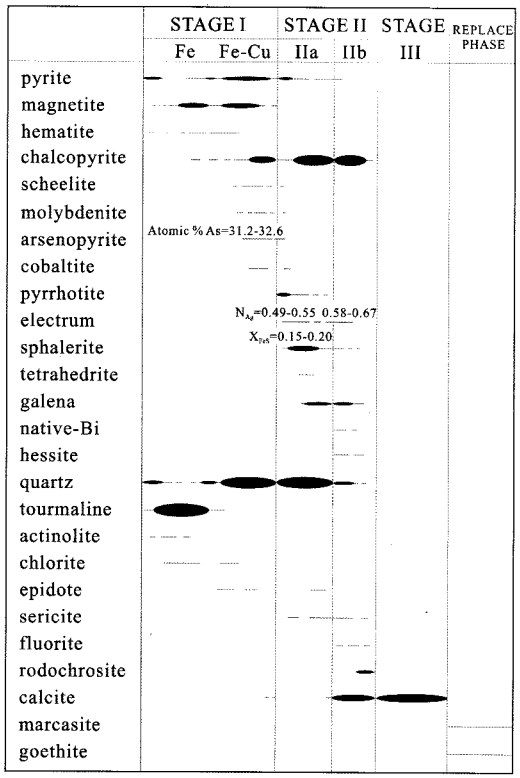

Fig. 2. Generalized paragenetic sequence of minerals from veins of the Haman area (after Heo *et al.*, 2003). Width of lines corresponds to relative abundance.

pyrite and chalcopyrite, with minor scheelite, molybdenite, arsenopyrite and cobaltite. Massive tourmaline and quartz often contain banded Fe-oxide and sulfide minerals with minor scheelite. Successive mineralic bands show a characteristic paragenetic sequence: tourmaline (± pyrite); a magnetite ore band; tourmaline + magnetite + pyrite + chalcopyrite; quartz + chalcopyrite ± scheelite and molybdenite.

Stage II contains the economically most significant mineralization and can be subdivided into two substages: base metal (IIa) and Cu-sulfide + carbonates (IIb). Base metal mineralization (IIa) is the most significant stage of sulfide mineralization as pyrite, arsenopyrite, pyrrhotite, chalcopyrite, sphalerite and galena with some sulfosalts. Pyrite is generally medium grained and occurs as subhedral to anhedral massive aggregates intergrown with, and replaced by chalcopyrite and sphalerite along fractures. Other fractures in pyrite are infilled by pyrrhotite and chalcopyrite. Infrequent coarse-grained arsenopyrite occurs in pyrite. Pyrrhotite is the major sulfide of ore and occurs as polycrystalline aggregates of anhedral grains containing (or intergrown with) chalcopyrite and other later ore minerals of the stage. It is often replaced by marcasite as a "bird's eye" texture. Some pyrrhotite occurs as a massive band near vein margins of the stage. Fine-grained electrum (49-67 atomic % Ag) occurs intimately intergrown with pyrrhotite, chalcopyrite and sphalerite. Ag contents of electrum show increase with time and mineral assemblage, from 49-55 atomic %, in electrum with pyrrhotite, to 58-67 atom % in electrum with chalcopyrite and sphalerite. Sphalerite (14.8-20.4 mole % FeS) forms anhedral to subhedral grains intergrown with chalcopyrite, galena and pyrite. Some sphalerite contains oriented rows of inclusions of chalcopyrite. Later sphalerite is intergrown with galena and sulfosalts, replacing pyrite or pyrrhotite. Anhedral galena occurs along grain boundaries or filling fractures in pyrite, pyrrhotite, chalcopyrite and sphalerite and rarely contains tetrahedrite. Native bismuth and hessite occur mainly within grains or filling fractures of pyrrhotite and rarely replace chalcopyrite. Cu-sulfide + carbonates mineralization (IIb) is characterized by white calcite, lesser amounts of fluorite and rhodochrosite, and minor white quartz. Chalcopyrite and minor sulfides and sulfosalts occur in calcite.

At the end of stage II mineralization, renewal of tectonic activity caused more faulting and brecciation. New fractures and openings were filled by economically barren massive calcite (stage III).

4. Geochemical Environments of Ore Mineralization

It is possible to constrain the chemistry of ore-forming fluids in the Haman area using observed mineral assemblages, chemical compositions, fluid inclusion and thermodynamic data.

Fluid inclusion and stable isotope data of the Haman mineralized area have been published (Heo *et al*, 2003). In this section, I summarize the results for calculating the chemical changes of the hydrothermal fluids at the area.

The ore and gangue mineral paragenesis at the Haman mineralized area can be divided into three distinct stages: Stage I, tourmaline + quartz + Fe-

Cu ore mineralization; Stage II, quartz + sulfides + sulfosalts + carbonates; Stage III, barren calcite. Earliest fluids are recorded in stage I and early portions of stage II veins as hypersaline (35-70 equiv. wt. % NaCl ± KCl) and vapor-rich inclusions which homogenize from ≈ 300° to ≥ 500°C. The high-salinity fluids are complex chloride brines with significant concentrations of sodium, potassium, iron, copper, and sulfur, though sulfide minerals are not associated with the early mineral assemblage produced by this fluid. Later solutions circulated through newly formed fractures and reopened veins, and are recorded as lower-salinity (less than ≈ 20 equiv. wt. % NaCl) fluid inclusions which homogenize primarily from ≈ 200° to 400°C.

Ranges of temperature and fugacity of sulfur (fs_2) were estimated from phase relations and mineral compositions in the systems Fe-As-S (Kretschmar and Scott, 1976), Au-Ag-S (Barton and Toulmin, 1964), Fe-Zn-S (Scott and Barnes, 1971) and Fe-O-S (Helgeson, 1969) and are shown in Figure 3.

Late magnetite of stage I is associated closely with pyrite, arsenopyrite and chalcopyrite in stage I mineralization. The mineral assemblage and the As contents of arsenopyrite (32.6 to 31.2 atomic percent) during stage I indicate temperatures of 450° to 355°C, which correspond to log fs_2 values of -5.5 to -8.7 bars (Fig. 3).

During stage IIa, early pyrite + pyrrhotite + electrum + sphalerite are followed by late pyrite + electrum + sphalerite + galena. The environment of stage IIa mineralization lies on or near the pyrite-pyrrhotite reaction curve (Fig. 3). The Ag contents of electrum increase from 49-55 (early) to 58-67 (late) atomic % Ag during stage IIa, whereas sphalerite of the stage IIa has a constant range of FeS contents between 20.4 and 14.8 mole percent from early to late stage IIa. These data indicate that the early and late mineral assemblages in stage IIa were precipitated within temperature ranges of 390° to 320°C and 355° to 270°C, respectively, which correspond to log fs_2 values of -7.5 to -9.6 and -8.8 to -11.7 bars, respectively (Fig. 3).

Native bismuth (bismuthinite does not occur), associated with sphalerite + galena + sulfosalts in stage IIb, restricts the upper limits of temperature and fs_2 to < 280°C and < $10^{-12.2}$ bars, respectively (Fig. 3).

The previously mentioned equilibrium thermodynamic and fluid inclusion data combined with mineral paragenesis indicate that copper minerals precipitated mainly within a temperature range of 350° to 250°C, which corresponds to log fs_2 values of -8.4 to -13.1 bars (Fig. 3).

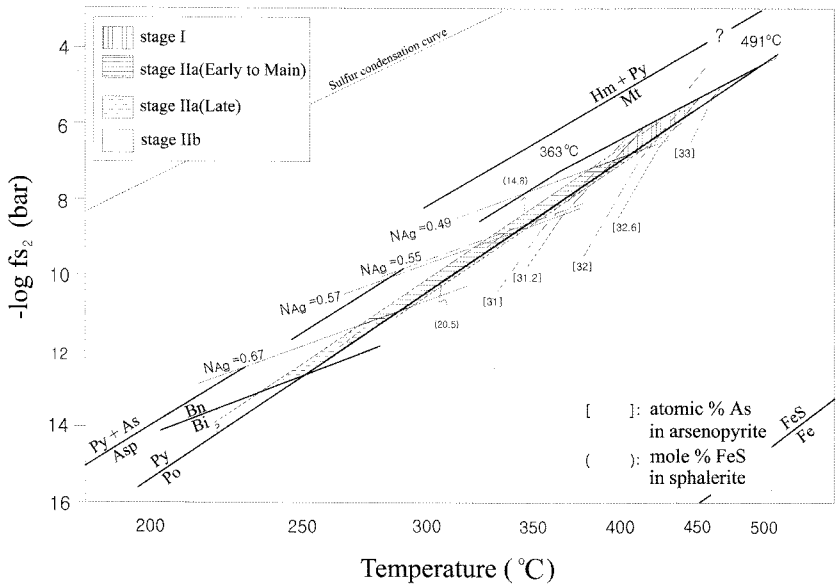

Fig. 3. Temperature versus fugacity of sulfur (fs_2) diagram showing the possible mineralization conditions for stage I and II from Haman area. Filled circles represent calculated T-fs_2 conditions for the mineral assemblage of electrum-pyrrhotite-sphalerite-pyrite in stage IIa quartz.

It is further possible to define chemical changes responsible for mineral deposition by using fugacity of sulfur (fs_2) versus fugacity of oxygen (fo_2) diagrams (Figs. 4 and 5). The diagrams, for convenience, have been constructed for 350° and 250°C in order to compare the chemical changes in pre- and post-main copper mineralization of stage II. Using Henry's law constant for 2.4 and 1.5 molar NaCl solutions (estimated by fluid inclusion data) at 350°C and 250°C (K = 7,400 and 7,900, respectively; Ellis and Golding, 1963) and assuming that

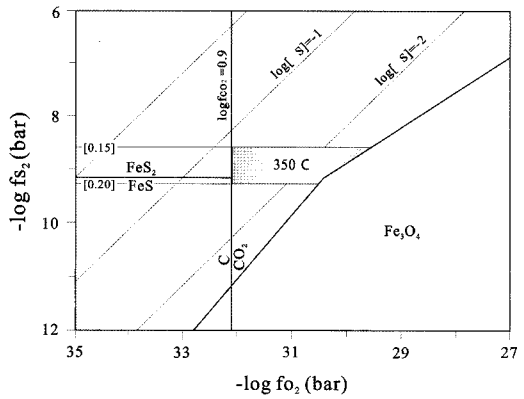

Fig. 4. Log fo_2-fs_2 diagram calculated at 350°C showing stability relationship of pre-main copper mineralization temperature. The ranges in fs_2 were calculated from the FeS content in sphalerite (Scott and Barnes, 1971) and mineral assemblages.

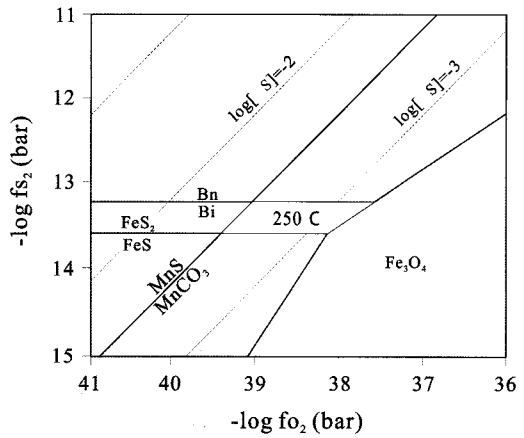

Fig. 5. Log fo_2-fs_2 diagram calculated at 250°C showing stability relationships of post-main copper mineralization temperature. The ranges in fs_2 were calculated from the FeS content in sphalerite (Scott and Barnes, 1971) and mineral assemblages.

Xco_2 was less than 0.001 (based on the typical absence of either liquid CO_2 or CO_2 hydrate in fluid inclusions), the probable log fco_2 values at 350°C and 250°C are estimated to be about 0.90 and 0.87 bars, respectively.

The occurrence of the assemblage pyrite + pyrrhotite + sphalerite and the absence of graphite and magnetite in early stage II mineralization (at ≈ 350°C) allow reconstruction of maximum and minimum values of log fo_2 of ≈ -29.9 and -32.1 bars, respectively (Fig. 4). The absence of magnetite and bismuthinite in late stage II mineralization (at ≈ 250°C) indicates that the maximum value of log fo_2 was < -37.7 bars. The minimum value of log fo_2 during the late mineralization (at ≈ 250°C) of stage II may be estimated from the occurrence of rhodochrosite and absence of alabandite. Assuming a log fco_2 value of 0.87 bars, the minimum log fo_2 value for the late mineralization (at ≈ 250°C) of stage II is approximately -39.3 bars (Fig. 5). The prevailing presence of sericite as the stage II vein-related alteration mineral (related to main mineralization) can be used to estimate the pH of hydrothermal fluids at 350°C (for pre-copper mineralization) and 250°C (for post-copper mineralization), respectively. The pH of the hydrothermal fluids at 350°C and 250°C in Haman area was controlled by kaolinite-sericite and sericite-quartz-K-feldspar reactions (Helgeson, 1969). The activities of K^+ were estimated using the temperature dependence of Na/K ratios for natural waters (Fournier and Truesdell, 1973) combined with the salinities (2.4 molar NaCl for 350°C and 1.5 molar NaCl for 250°C) of each fluid and activity coefficients for K^+ (calculated from the Debye-Hückel equation). Probable pH ranges of fluids at 350° and 250°C (defined by the sericite stability) are about 3.6 to 4.9 and 4.3 to 5.3, respectively. These data, coupled with the log fo_2 values at each temperature, are used to estimate variations in copper solubility.

Utilizing solubility data from Crerar and Barnes (1976) for chloride complexes, contours of copper solubility (ppm) in solution have been plotted in Figure 6. During early mineralization at 350°C (pH range = 3.6 to 4.9; log fo_2 range = -29.9 to -32.1) significant amounts of copper (10^3 to 10^2 ppm) could be dissolved in weakly acid NaCl solutions. For late mineralization at 250°C (pH =

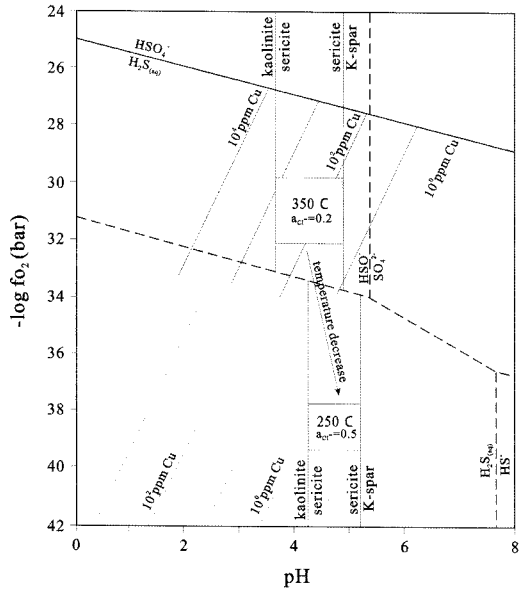

Fig. 6. Solubility of the cuprous complex (CuCl) in a solution at equilibrium with chalcopyrite + pyrite (+ bornite) as a function of pH and oxygen fugacity, modified from Crerar and Barnes (1976). The solid and dashed lines represent stability boundaries and Cu solubilities at 350°C and 250°C, respectively.

4.3-5.3; $\log f_{O_2}$ = -37.7 to -39.3) about 10^0 to 10^{-1} ppm copper could be dissolved. From Figure 6, a maximum concentration of copper exceeding 10^3 ppm could be transported as chloride complex at 350°C. Cooling of the fluid to 250°C would have precipitated almost all of the dissolved copper (Romberger and Barnes, 1970; Crerar, 1974; Crerar and Barnes, 1976). Copper deposition in the Haman hydrothermal systems was likely a result of a progressively decreasing temperature, and the changes in chemical conditions (f_{S_2}, f_{O_2}, pH, etc.) resulting in decrease of solubility of copper chloride complexes.

5. Summary

The ore mineralization of the Gunbuk, Jeilgunbuk, and Haman deposits in the Haman mineralized area is contained within three distinct stages of quartz and calcite veins which were separated in time by tectonic events marked by fracturing and brecciation.

Fluid inclusion evidence suggests that early (stage I and eary portion of stage II) vein minerals were deposited at temperatures between ≥ 500° and ≈ 300°C from hypersaline fluid and heated meteoric waters. Fluid inclusion data from post-ore carbonate stage mineralization reflect much cooler (≈ 200°C).

Late mineralization of stage I, which is characterized by magnetite associated closely with pyrite, arsenopyrite and chalcopyrite, occurred at temperatures of 450° to 355°C, which correspond to log f_{S_2} values of -5.5 to -8.7 bars. The early (pyrite + pyrrhotite + electrum + sphalerite) and late (pyrite + electrum + sphalerite + galena) mineral assemblages in stage IIa were precipitated within temperature ranges of 390° to 320°C and 355° to 270°C, respectively, which correspond to log f_{S_2} values of -7.5 to -9.6 and -8.8 to -11.7 bars, respectively. Native bismuth (bismuthinite does not occur), associated with sphalerite + galena + sulfosalts in stage IIb, restricts the upper limits of temperature and f_{S_2} to < 280°C and < $10^{-12.2}$ bars, respectively.

The mineralogy and chemistry in early stage II mineralization (pyrite + pyrrhotite + sphalerite; at ≈ 350°C) and late stage II mineralization (the absence of magnetite and bismuthinite, and the occurrence of rhodochrosite and absence of alabandite; at ≈ 250°C) show the values of log f_{O_2} from ≈ -29.9 to -32.1 bars and from < -37.7 bars to -39.3 bars, respectively.

The previously mentioned equilibrium thermodynamic and fluid inclusion data combined with mineral paragenesis indicate that copper minerals precipitated mainly within a temperature range of 350° to 250°C. The pH of the hydrothermal fluids at 350°C and 250°C in Haman area was controlled by kaolinite-sericite and sericite-quartz-K-feldspar reactions. Probable pH ranges of fluids at 350° and 250°C are about 3.6 to 4.9 and 4.3 to 5.3, respectively. During early mineralization at 350°C, significant amounts of copper (10^3 to 10^2 ppm) could be dissolved in weakly acid NaCl solutions. For late mineralization at 250°C, about 10^0 to 10^{-1} ppm copper could be dissolved.

Equilibrium thermodynamic interpretation indicates that the copper in the Haman systems could have been transported as a chloride complex and the copper precipitation occurred as a result of cooling accompanied by changes in the geochemical environment (f_{S_2}, f_{O_2}, pH, etc.) resulting in

decrease of solubility of copper chloride complexes.

Acknowledgements

This work was supported by the research grant of the Chungbuk National University in 2008.

References

Barton, P.B. Jr. and Toulmin, P.III. (1964) The electrum-tarnish method for the determination of the fugacity of sulfur in laboratory sulfides system. Geochim. Cosmochim. Acta, v. 28, p.619-640.

Choi, S.H., So, C.S., Kweon, S.H. and Choi, K.J. (1994) The geochemistry of copper-bearing hydrothermal vein deposits in Goseong mining district (Samsan area), Gyeongsang basin, Korea. Econ. Environ. Geol. v. 27, p. 147-160.

Choi, S.H., So, C.S., Youm, S.J. and Shelton, K.L. (1998) Geochemistry and genesis of hydrothermal Cu deposits in the Gyeongsang Basin, Korea: Masan mineralized area. N.Jb.Miner. Anh., V.173, p. 189-206.

Crerar, D.A. (1974) Solvation and deposition of chalcopyrite and chalcocite assemblages in hydrothermal solution. - Ph D. dissertation, Dept. of Geological Sciences, The Pennsylvania State University.

Crerar, D.A. and Barnes, H.L. (1976) Ore solution chemistry V. Solubilities of chalcopyrite and chalcocite assemblages in hydrothermal solution at 200°C to 350°C. Econ. Geol., v, 71, p. 772-794.

Ellis, A.J. and Golding, R.M. (1963) The solubility of carbon dioxide above 100°C in water and in sodium chloride solutions. Am. Jour. Sci., v 261, p. 47-60.

Fournier, R.O. and Truesdell, A.H. (1973) Am empirical Na-K-Ca geothermometer for natural waters. Geochim. Cosmochim. Acta, v. 73, p. 1255-1275.

Hegelson, H.C. (1969) Thermodynamics of hydrothermal systems at elevated temperatures and pressures. Am. Jour. Sci. v. 26, p.729-804.

Heo, C.H., Yun, S.T., So, C.S., Choi, S.H. and Youm, S.J. (2001) Complex geochemical evolution of hydrothermal fluids related to breccia pipe Cu-W mineralization of the Dalseong mine, Korea. N.Jb.Miner.Abh., v. 176, p. 127-151.

Heo, C.H., Yun, S.T., Choi, S.H., Choi, S.G. and So, C.S. (2003) Copper mineralization in the Haman-Gunbuk Area, Gyeongsangnamdo-Province: Fluid inclusion and stable isotope study. Econ. Environ. Geol., v. 36, p. 75-87.

Jin, M.S., Lee, S.M., Lee, J.S. and Kim, S.J. (1982) Lithochemistry of the Cretaceous granitoids with relation to the metallic ore deposits in Southern Korea. Jour. Geol. Soc. Korea , v. 18, p. 119-131.

Kretshmar, U. and Scott, S.D. (1976) Phase relations involving arsenopyrite in the system Fe–As–S and their application. Canadian Mineralogists, v.14, p.364-386.

Romberger, S.B. and Barnes, H.L. (1970) Ore solution chemistry III. Solubility of CuS in sulfide solutions. Econ. Geol. v. 65, p. 901-919.

Sato, K., Shtmazaki, H. and Chon, H.T. (1981) Sulfur isotopes of the ore deposits related to felsic magmatism in the southern Korean Peninsula. Mining Geology, v.31, p. 321-326.

Scott, S.D. and Barnes, H.L. (1971) Sphalerite geothermometry and geobarometry. Econ. Geol., v.66, p.653-669.

Sillitoe, R.H. (1980) Evidence for porphyry-type mineralization in Southern Korea. Mining Geology Spec. Issue 8, p. 205-214.

So, C.S., Chi, S.J. and Shelton, K.L. (1985) Cu-bearing hydrothermal vein deposits in the Gyeongsang Basin, Republic of Korea. Econ. Geol., v. 80, p. 43-56.

So, C.S., Choi, S.H. and Shelton, K.L. (1997) Geochemistry and genesis of hydrothermal Cu deposits in the Gyeongsang Basin (Andong area): A link between porphyry and epithermal systems. N.Jb.Miner.Abh., v. 171, p. 281-307.

Yun, S.T., Choi, S.H. and So, C.S. (1996) Complex geochemical evolution of hydrothermal fluids related to polymetallic Cu-Zn-Pb mineralization of the Namseon mine, Gyeongsang Sedimentary Basin, Korea. N.Jb.Miner.Abh., v. 170, p. 127-153.

2009년 1월 9일 원고접수, 2009년 2월 20일 게재승인